MicroGPS for Low-Cost Orbit Determination

S. C. Wu, W. I. Bertiger, D. Kuang, S. M. Lichten, S. Nandi, L. J. Romans, and J. M. Srinivasan
Tracking Systems and Applications Section

This article presents a new technology for satellite orbit determination using a simple Global Positioning System (GPS) receiver (microGPS) with ultra-low cost, power, and mass. The capability of low-cost orbit determination with microGPS for a low Earth-orbiting satellite, Student Nitric Oxide Explorer (SNOE), is demonstrated using actual GPS data from the GPS/Meteorology (MET) satellite. The measurements acquired by the microGPS receiver will be snapshots of carrier Doppler and ambiguous pseudorange. Among the challenges in orbit determination are the resolution of the pseudorange ambiguity; the estimation of the measurement time tag drift, which affects the in-track orbit position solution; and the convergence of the orbit solution from a cold start with essentially no knowledge of the orbit. The effects of data gaps and Doppler data quality are investigated. An efficient data acquisition scenario for SNOE is derived.

I. Introduction

Global Positioning System (GPS) measurements can provide precise positioning for users on Earth and in Earth orbits. Positioning to 1-cm accuracy has been reported for users on Earth [1,2] and to 2 cm for a user in a low Earth orbit [3,4]. Such high-precision positioning requires a state-of-the-art GPS receiver on board to acquire precise GPS carrier phase and/or pseudorange data to be processed with ground data from a network of tracking sites over a period of time. Such full-blown onboard receivers are not only costly, but also heavy and power hungry.

Many NASA, military, and commercial satellite programs have a need for tracking systems with ultra-low power, mass, and cost for medium-accuracy (a few hundred meters) orbit determination of small, low Earth-orbiting satellites. The Jet Propulsion Laboratory (JPL) and the University of Colorado have collaborated to develop a tracking system using a novel GPS technology, to be called microGPS.

Two missions are scheduled to carry a microGPS receiver. The first is the Student Nitric Oxide Explorer (SNOE) mission, to be launched in October 1997. It will have a 550-km circular orbit with a goal of 200-m orbit determination accuracy. The second is the Space Technology Research Vehicle (STRV-1C) mission, to be launched in early 1999. It will have a highly elliptical orbit with a goal of characterizing GPS signal strength from 300 km to geosynchronous orbit altitudes.

The onboard microGPS receiver is basically a "bit grabber," consisting of one or more GPS patch antennas, an inexpensive oscillator, a signal sampler/downconverter, and a memory chip. Such a receiver will not only fulfill stringent power (<0.1-W) and mass (<1-kg) constraints, but with the inclusion of an onboard processor, potentially could offer autonomous tracking capability. The microGPS requires

very low power because it only occasionally awakes from a "sleep" mode to sample GPS signals for a short duration. The measurements acquired by the microGPS receiver are carrier Doppler and ambiguous pseudorange, with an ambiguity of 1 ms (∼300 km). Among the challenges in orbit determination are the resolution of the pseudorange ambiguity; the determination of the measurement time tag, which could drift off by many seconds; and the convergence of the orbit solution from a cold start with poor a priori knowledge of the orbit.

This article reports on the processing procedure and the estimation scheme as well as the results of a demonstration for the SNOE satellite using the actual space GPS data from the GPS/Meteorology (MET) satellite [5]. The Real-Time Gipsy (RTG) software system [6] developed at JPL is used for the analysis. Based on the results of this demonstration, an efficient data-taking scenario is derived. The maximum data gap beyond which convergence of the orbit solution may not be realized is determined.

II. MicroGPS Flight Hardware

The current trend in Earth orbiters is toward microspacecraft that perform their science and/or engineering tasks autonomously (fire-and-forget missions). In this scenario, onboard power and mass are premium resources. GPS receivers have and will continue to play important roles in these small spacecraft, providing navigation and attitude data in light and low-power modules (see Table 1). The motivation for developing the microGPS technique was to further reduce mass and power while improving reliability over current GPS flight receivers. The microGPS flight receiver accomplishes this by employing a new tracking paradigm we call sparse sampling and by shifting all signal-processing functions from dedicated hardware to flexible, portable software.

Table 1. Current GPS receivers with flight experience and the microGPS.

Receiver	Qualification	No. of satellites (frequency)	Mass, kg	Power, W
Rockwell	Space	5 (L1)	2.3	6.0
Motorola Viceroy	Space	12 (L1)	1.5	4.8
Trimble Tans Quadrex	Commercial	6 (L1)	1.5	3.5
AOA TurboStar	Commercial	8 (L1/L2)	1.5	4.0 (L1) 7.0 (L1/L2)
Rockwell	Space	10 (L1/L2)	2.6	16
Loral Tensor	Space	8 (L1/L2)	4	15
MicroGPS[a]	Commercial/ space (planned)	No limit (L1/L2)	0.5	0.05 average, 1 peak

[a] MicroGPS parameters do not include an onboard flight computer.

The microGPS receiver consumes less power than typical flight GPS receivers because it uses a sparse sampling technique in which the receiver awakens and acquires GPS data only periodically, remaining "asleep" between samples. When combined with software possessing accurate dynamic models, these snapshots of the GPS constellation can produce accurate orbits. The microGPS receiver is lighter than typical flight GPS receivers because it uses a modified hardware/software architecture in which all GPS-specific signal processing typically implemented in hardware has been moved to software (see Fig. 1).

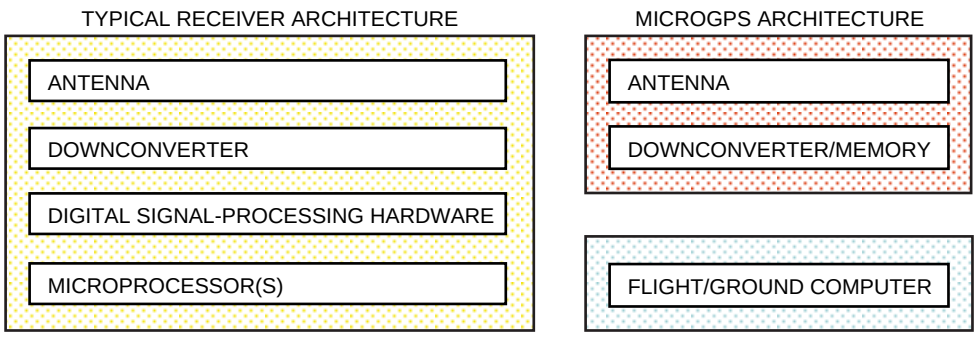

Fig. 1. Receiver architecture comparison.

The microGPS receiver is more reliable than typical commercial flight receivers because of several factors. The hardware parts count has been greatly reduced, with most of the lowest-reliability part types of typical flight receivers eliminated. Furthermore, sparse sampling calls for only brief power-on periods with frequent power cycling on most of the hardware in the microGPS, providing added protection against some destructive radiation effects. In addition, in the microGPS architecture, the computer that executes this software can physically be at any location that is in periodic communication with the spacecraft. For the first two missions that will carry a microGPS, SNOE and STRV, the computer will be on the ground. For future missions, we plan to migrate the modular software to reside on board, executed by either a special purpose microprocessor in the microGPS or by the spacecraft flight computer.

We anticipate that fully space-hardened microGPS flight units probably will cost a few tens of thousand dollars each, at least an order of magnitude less than typical space-qualified commercial GPS flight receivers.

The microGPS acquires and stores snapshots of raw GPS signal at a programmable rate (typically a few times per orbit). In addition, individual snapshots can be single, short-duration samples (typically a few milliseconds) or bursts of samples whose number and sample spacing also are programmable. During the data acquisition period (usually a few milliseconds), the microGPS consumes a peak power of about 1 W. Between data snapshots, the microGPS draws a very small quiescent current. During the brief transfer of the GPS signal samples to the onboard flight computer, the receiver will require 0.5 W. The raw GPS signal samples are time tagged by the microGPS's real-time clock and then transferred to the flight computer. These transfers can occur at a convenient rate constrained by the depth of the instrument memory and the rate of the data transfer. Once they are received by the flight computer, the GPS sample bits will be stored for later transmission to the ground (and subsequent ground processing, as planned for SNOE and STRV) or processed in real or near-real time by onboard software.

III. MicroGPS Flight Tests

Two missions will carry a microGPS receiver in the next 2 years. The data collected by these instruments will be processed by the algorithms described in this article to produce orbit solutions for low Earth and highly elliptical orbiters.

A. SNOE Mission

The first mission to use the microGPS technology is the Student Nitric Oxide Experiment (SNOE). It is a Student Explorer Demonstration Initiative (STEDI) mission funded by NASA through the University Space Research Association (USRA). The small scientific spacecraft has been designed and built and will be operated entirely at the University of Colorado, Laboratory for Atmospheric and Space Physics (CU/LASP), and will be launched into a Sun-synchronous 550-km orbit at a 97.5-deg inclination. SNOE will carry the first microGPS instrument, whose development is a NASA-sponsored joint effort between

JPL and the Colorado Center for Atmospheric Research (CCAR). SNOE currently anticipates a Pegasus launch scheduled for October 1997.

The goal of SNOE's microGPS will be to determine the SNOE orbit to within 200 m. The nominal data-sampling time is 2 ms, with only a few samples taken per orbit. The data volume will be a few hundred kbytes per day. The overall weight of the SNOE receiver will be about 0.6 kg. The power consumption will be <0.1 W on average and <1 W at peak.

B. STRV-1C Mission

The Space Technology Research Vehicle (STRV-1C) is the third in a planned series of four spacecraft designed to evaluate new technologies that have application to future space missions. Developed by the British Defence Research Agency (DRA), STRV-1A and -1B were launched in June 1994, and STRV-1C is scheduled for an early-1999 launch into a geostationary transfer orbit (GTO). A dual-frequency microGPS receiver will be carried on STRV-1C, whose development is jointly sponsored by NASA, the U.S. Department of Defense, and the DRA.

The goal of STRV's microGPS will be to characterize the GPS signals from 300 km up to geostationary altitudes. At a geostationary orbit, since the receiver will be at a higher altitude than the GPS satellites, the microGPS will rely on the fact that radiation from current GPS satellites on the far side of the Earth (relative to STRV) actually spills past the Earth's limb and will illuminate STRV. In addition, because it is actually in a GTO, any side- and back-lobe radiation patterns of the GPS satellites also will be measured. The nominal data-sampling time is 20 ms. Many samples will be taken per orbit, with a data volume of up to 20 Mbytes per day. The overall weight of the receiver is expected to be about 0.9 kg. The power consumption will be <0.25 W on average and <3 W at peak.

IV. Ambiguity Resolution of GPS Pseudorange Data

The simplicity of the microGPS receiver precludes the acquisition of common GPS data types, namely, carrier phase and pseudorange. Instead, the data types available are carrier Doppler and ambiguous pseudorange with an ambiguity of 1 ms (∼300 km). These data types, acquired at a few time points, are not sufficient for orbit determination even at the kilometer level. However, the pseudorange ambiguity can be resolved easily with the help of the Doppler data, promoting the ambiguous pseudorange into a far stronger data type.

The resolution of pseudorange ambiguity is done in two steps. First, a crude orbit solution accurate to 20 to 50 km is determined with the Doppler data at two epochs separated by a few minutes. Measurements at two epochs are crucial since Doppler data at a single epoch contain only information of orbit velocity. Next, a crude but unambiguous pseudorange data set is computed based on this crude orbit and the known (to a far better accuracy) GPS orbits. The accuracy of these computed pseudorange measurements, which is better than 50 km, is well within the 300-km pseudorange ambiguity. This facilitates the resolution simply by direct comparison of these computed pseudorange measurements with the actual ambiguous pseudorange measurements. The process, in the presence of user clock error, is described in the following paragraphs.

For convenience, let the unit of pseudorange be ms so that the ambiguity cycle is of unit value. Similarly, let Doppler be in ms/s and clock bias be in ms. Let $R_1(frac), R_2(frac), \ldots, R_n(frac)$ be the ambiguous pseudorange measurements, i.e., each $R(frac)$ is the fractional part of the pseudorange, which also includes the clock bias and data noise.

The ambiguity-free pseudorange measurements can be written as

$$\left.\begin{aligned} R_1 &= R_1(frac) + N_1 + M \\ R_2 &= R_2(frac) + N_2 + M \\ &\vdots \\ R_n &= R_n(frac) + N_n + M \end{aligned}\right\} \tag{1}$$

where the last two terms in each line are the integer part of the geometrical range and user clock bias, respectively, with N and M being unknown integers.

A crude user orbit and time-tag bias are determined with GPS Doppler measurements. A few iterations may be required if the initial orbit error is large. From this crude orbit, one can calculate the geometrical ranges $R_1(dop), R_2(dop), \ldots, R_n(dop)$. The crude but unambiguous pseudorange measurements can be expressed in terms of the Doppler inferred geometrical ranges as

$$\left.\begin{aligned} R_1 &= R_1(dop) + M + C \\ R_2 &= R_2(dop) + M + C \\ &\vdots \\ R_n &= R_n(dop) + M + C \end{aligned}\right\} \tag{2}$$

where the last two terms account for the integer and fractional parts of the user clock bias. These crude pseudorange data are comparable in accuracy to the crude orbit determined with GPS Doppler measurements.

Subtracting Eq. (1) from Eq. (2), determine $N_1 - C, N_2 - C, \ldots, N_n - C$ as real numbers:

$$\left.\begin{aligned} B_1 &= N_1 - C = [R_1(dop) - R_1(frac)] \\ B_2 &= N_2 - C = [R_2(dop) - R_2(frac)] \\ &\vdots \\ B_n &= N_n - C = [R_n(dop) - R_n(frac)] \end{aligned}\right\} \tag{3}$$

Note that B differs from integers by C, the fractional part of the user clock bias; but this is common to all B's. Such common bias does not complicate final orbit determination since a user clock bias is estimated in common practice.

The criterion for successful ambiguity resolution is for the fractional part of B to cluster within a finite bound. In the following analysis, a bound of ± 0.15 will be adopted. This is equivalent to a 90-km scatter for the crude pseudorange error as calculated in Eq. (2). If the fractional part of $B_1, B_2, \ldots, B_n$ clusters around 0.5, calculate the average of the fractional part of all $B_1, B_2, \ldots, B_n$. Deducting this average from all $B_1, B_2, \ldots, B_n$ moves them close to integers, and they easily can be rounded to those integers to yield $N_1, N_2, \ldots, N_n$. These integers may have a *common* error of not greater than 1 due to the fractional part of the user clock bias C.

The geometrical range ambiguity can now be removed by respectively adding $N_1, N_2, \ldots, N_n$ to $R_1(frac), R_2(frac), \ldots, R_n(frac)$:

$$\left.\begin{aligned} R_1(frac) + N_1 &= R_1(geom) + C \\ R_2(frac) + N_2 &= R_2(geom) + C \\ &\vdots \\ R_n(frac) + N_n &= R_n(geom) + C \end{aligned}\right\} \tag{4}$$

where $R(geom)$ is the ambiguity-resolved geometrical range while $R(geom) + C$ is the ambiguity-resolved pseudorange.

V. Separation of Time-Tag Bias From Pseudorange Bias

The ambiguity-resolved pseudorange data can be used together with the Doppler data for final orbit determination. The pseudorange data are corrupted by the (fractional part of) the user clock bias, and Doppler data are corrupted by the user frequency bias. Furthermore, a time-tag bias would also affect both data types. To remove the effects of user clock errors, a clock bias and a frequency bias should be estimated together with the orbit elements.

It is a common practice to assume that time-tag bias is consistent with pseudorange bias and can be adjusted in the filtering process as a common parameter, if needed. This is indeed true with conventional GPS (unambiguous) pseudorange measurements. However, the assumption is invalid with ambiguous pseudorange data acquired with a microGPS receiver, even after resolving the ambiguity: While the time-tag bias could approach the full clock error (as large as seconds), the clock bias on the ambiguity-resolved pseudorange data is limited to its ambiguity cycle, 1 ms [cf., Eq. (4)].

If a common clock bias parameter is used to represent both time-tag bias and pseudorange bias, the measurement of partial derivatives with respect to this parameter is dominated by the pseudorange bias, which has a value of 3×10^5 km/s (the speed of light) as compared with the few-km/s contribution from the time-tag offset. Solving for the time-tag offset using this parameter would yield a solution approaching the fractional user clock offset of <1 ms, which can be far off the actual time-tag offset. This would leave a km-level residual for every second of time-tag offset, which would alias into a few-km orbit solution error. Therefore, when the time-tag bias is being estimated, its partial derivative should be separated from that of the pseudorange bias. In other words, both parameters should be simultaneously adjusted in the filtering process with separate partial derivatives. A frequency bias also may be adjusted when Doppler data are involved.

VI. GPS/MET Demonstration

Without in-flight microGPS data before SNOE is put in orbit in October 1997, a demonstration with actual GPS data from a satellite of similar orbital characteristics would be highly desirable. Here, the GPS data acquired from a low Earth-orbiting satellite, GPS/MET [5], were adopted. GPS/MET has a circular orbit at a 715-km altitude and 70-deg inclination while SNOE will have a circular orbit at a 550-km altitude and 97-deg inclination. To perform atmospheric occultation experiments, GPS/MET orients its GPS receiver to be aft pointing, limiting the number of GPS satellites in view. The orbit determination from such suboptimal observing geometry should provide an upper bound estimate for SNOE orbit solution error with the microGPS.

Precise after-the-fact GPS ephemerides from a worldwide ground network tracking were used. However, only long-term linear drifts of the GPS clocks were corrected for; the effects of selective availability (SA) dithering were not taken out. The precise GPS/MET orbit solutions with differential GPS, believed to be accurate to better than 20 cm [5], were used as the truth for assessing the orbit determination accuracy.

To simulate a cold-start situation, very poor a priori orbit and clock were assumed: 500 km in orbit altitude, 2000 km in cross-track and in-track orbit position, 2 km/s in orbit velocity, 100 s in SNOE clock (time tag), and 1 μs/s in clock rate. GPS/MET data from two consecutive days, July 16–17, 1996, were used. The L1 pseudorange data were sampled at 15-, 30-, and 45-min intervals and converted into ambiguous pseudorange measurements by retaining only the fractional ms parts. L1 carrier phase data at consecutive time points separated by 10 s were differenced to form carrier Doppler measurements and then sampled at the same 15- to 45-min intervals. A random-walk user clock error was added onto these data and their time tags. Additional data noise also was added to investigate the effect on orbit convergence and accuracy.

The orbit determination algorithm first tries to obtain a crude orbit solution using only a single epoch of Doppler data to resolve the pseudorange ambiguities. If this fails, Doppler data at two epochs are collected to solve for the crude orbit and to resolve the pseudorange ambiguities. The effects of SA on the Doppler data are estimated to be about 0.3 m/s. The actual Doppler measurements from the microGPS receiver on SNOE are expected to have a higher data noise, $\sim$2 m/s. To account for this, white noise of different sizes was added to the Doppler data to simulate different levels of data noise. At each level of data noise, a total of six trials were made to investigate the data noise effects on orbit convergence (and hence successful pseudorange ambiguity resolution). These trials were taken by sampling two consecutive data points every 1 h.

The clock on board SNOE will be drifting and may have an offset from the GPS system clock by many seconds. This will affect the GPS measurements in two respects: First, a common pseudorange offset error will exist on measurements from all GPS satellites. Second, the data time tags also will have a common offset that translates into an in-track SNOE orbit error of $\sim$7.5 km for each second of time-tag error.

VII. The RTG Software System

A newly developed software system, the Real-Time Gipsy (RTG) [6], is used for the data processing. This software system is written in ANSI-C and is capable of processing general radio metric data types in real time on an onboard processor. The RTG also currently is in use for the Federal Aviation Administration's (FAA's) real-time GPS Wide-Area Augmentation System (WAAS). It is near its completion and is capable of processing microGPS data types as well as the usual GPS data types (phase and pseudorange). A numerical integrator is used to allow arbitrary extension of the dynamic models. A current-state, general process-noise UD factorized filter [7] is implemented in the RTG.

Currently, the RTG executes on Hewlett Packard (HP) workstations under UNIX, and on PCs. Its target platforms for the SNOE and STRV missions are ground-based Macintosh PowerPCs and HP9000 workstations. The software has been written in such a way that eventual migration to a real-time flight processor will be straightforward.

VIII. Results of the Demonstration

Figure 2 shows the success rate of orbit convergence during the six trials as a function of Doppler data noise. In general, two epochs of data are needed for the orbit to converge, except for one of the six trials at the lowest 2m/s data noise. A 15-min data separation works well for all data noise up to 15 m/s, while one trial with a 30-min data separation fails to converge. No solution will converge with a data separation

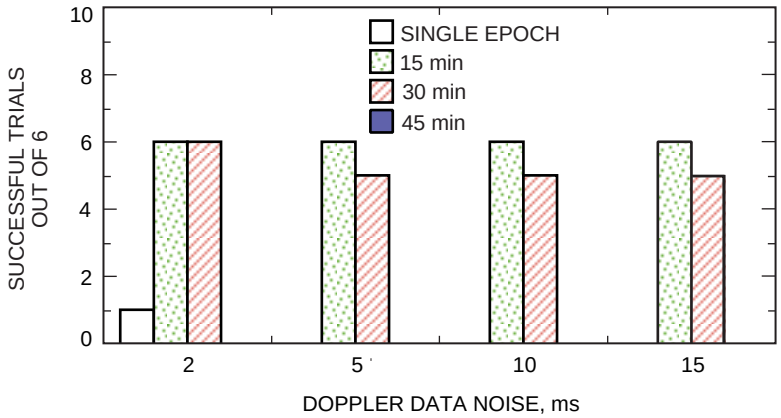

Fig. 2. The success rate of convergence of the Doppler inferred orbit.

of 45 min or longer. The need of Doppler data at two epochs can be explained by the formal error of the Doppler inferred orbit solution, as shown in Fig. 3. With a single epoch of data, the formal error is far greater than the ∼300-km pseudorange ambiguity. The error drops by almost 2 orders of magnitude with data at two epochs, even at a small separation of 3 min. At longer separations, the formal error remains at the same level, but the error due to mismodeled velocity and dynamics will dominate, keeping the orbit from converging with a data interval of 45 min or longer.

The three-dimensional (3-D) root-sum-square (RSS) error of the crude orbit solution for a 30-min data separation is shown in Fig. 4, again as a function of Doppler data noise. The error is calculated by differencing the Doppler inferred orbit solution from the truth orbit (the precise GPS/MET orbit). The error is lower than 50 km for a data noise of 5 m/s or better. Note that pseudorange ambiguity resolution was successful in one case when the crude orbit error was as large as 120 km.

As mentioned earlier, it is desirable to have a low data sampling interval in order to conserve power consumption and keep the data volume low. From the above analysis, it appears that a 30-min sampling interval is appropriate with 2-m/s Doppler data. With a higher Doppler noise, a smaller data interval may be needed at a cold start; thereafter, a longer interval can be used, as will be demonstrated in the following. This will require the receiver to wake up only a few times per orbit revolution. In the following analysis, a 2-m/s Doppler noise with a 30-min data-sampling interval will be assumed.

With two epochs of Doppler measurements, the orbit solution converges in a few iterations, as shown in Fig. 5. Here, the orbit position components are given in terms of the inertial coordinate system used in orbit integration.

Once the pseudorange ambiguities are resolved using a crude orbit determined from Doppler measurements, the resulting ambiguity-free pseudoranges were used to solve for precise orbit position and velocity. Although the information contained in Doppler measurements is much weaker than that contained in pseudorange measurements, the former also was included in the final solution with very little additional computational cost.

With two epochs of ambiguity-resolved pseudorange measurements, the precise orbit solution converges in one or two iterations, as shown in Fig. 6. The converged orbit position and time-tag solutions typically are better than 100 m and 20 ms, respectively. The orbit position will, in general, degrade with time due to the errors in orbit velocity and dynamic models. Without any modeling of the atmospheric drag, the orbit can drift away by as much as a few hundred meters in 30 min, when the next data batch is available. However, pseudorange ambiguity resolution is guaranteed at this level of orbit error even without the help of Doppler measurements. Therefore, once a converged orbit solution is obtained with the first two epochs

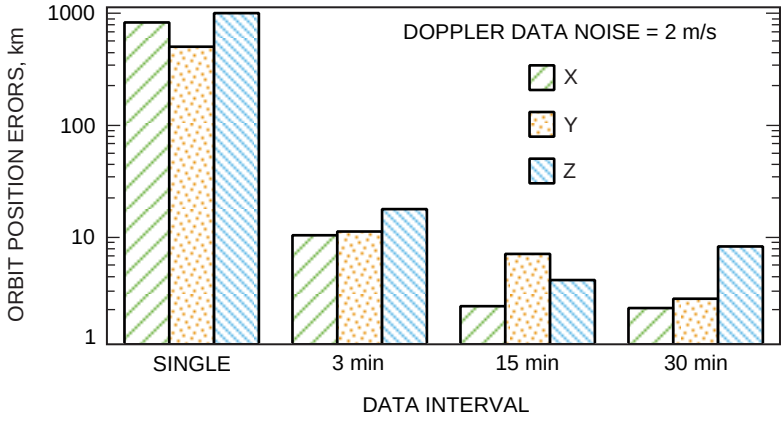

Fig. 3. Formal errors of the Doppler inferred orbit components.

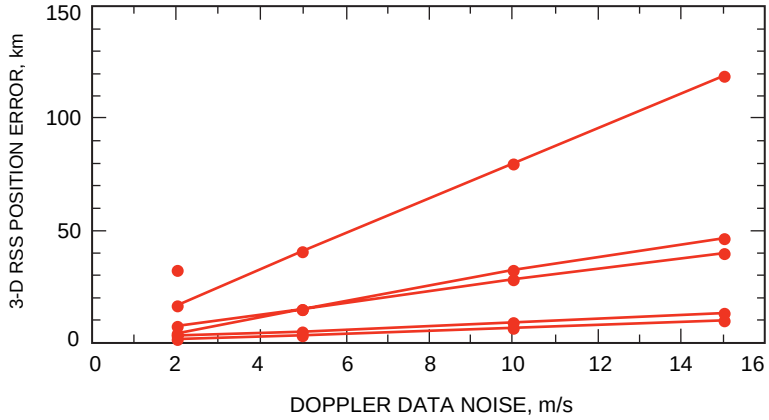

Fig. 4. Crude orbit solution error from two epochs of Doppler measurements separated by 30 min.

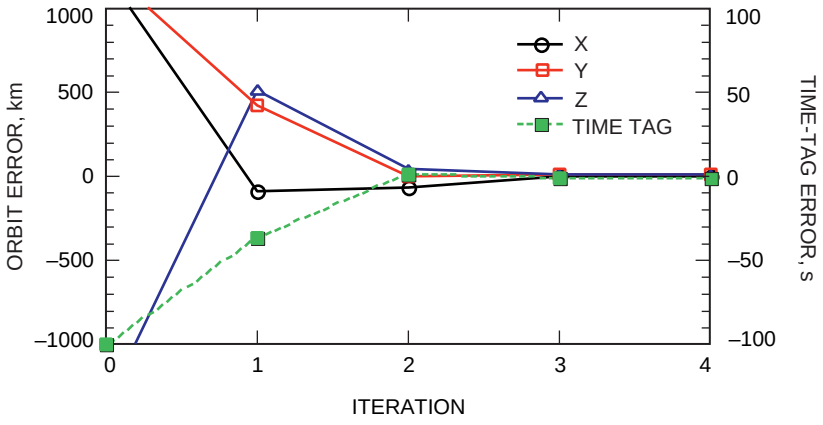

Fig. 5. Crude orbit convergence with Doppler measurements.

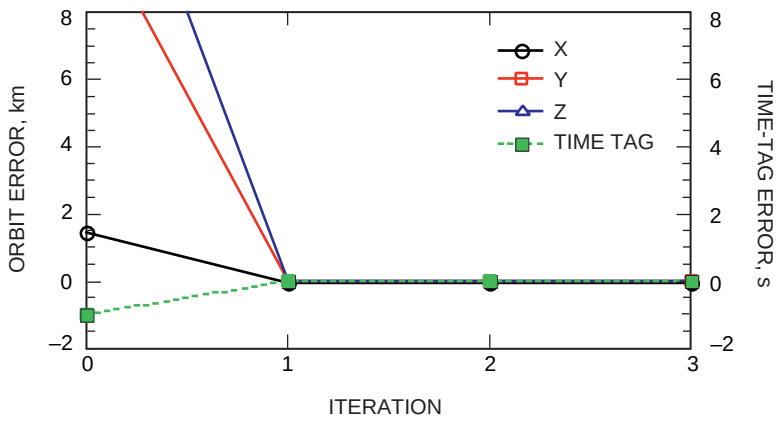

Fig. 6. Orbit convergence with pseudorange measurements.

of measurements (separated by 30 min), a single epoch of ambiguous pseudorange measurements alone will be sufficient to update the orbit every 30 min.

To demonstrate that snapshots of GPS measurements at epochs separated by 30 min are indeed sufficient to maintain the orbit to within a few hundred meters, two consecutive days of GPS/MET space-flight GPS data, of length 18 and 15 hours, respectively, were processed. Here, GPS Doppler and ambiguous pseudorange measurements were taken at 30-min intervals. A 2-m/s noise was added to the Doppler data and a 15-m noise to the pseudorange data (in addition to the ∼30-m SA error). A random-walk user clock drift at the level of 0.1 s every 30 min also was added to both data types. The treatment of all estimated parameters in the filter is summarized in Table 2. The 3-D orbit velocity components were treated as process-noise parameters to reduce the sensitivity to mismodeled dynamics. The quadratically added 0.54-cm/s velocity uncertainty at every data epoch is equivalent to a steady-state process-noise force of 3 μm/s^2.

The filter UD matrix, which contains the parameter estimates and their covariances, from the previous data batch was mapped to the new data epoch after adding the process noise listed in the last column of Table 2. The estimates then were used to update the nominal values of the measurement models and then reset to zero. This modified UD matrix then was efficiently combined with the UD matrix of the *converged* filter solutions resulting from processing the new data batch alone. This post-filter UD combining process is necessary to assure proper weighting between the previous UD matrix and the new data batch whenever an iteration process is involved. A cheaper way of combining the information would be

Table 2. Filter parameterization.

Parameter	Type	A priori noise	Noise added between epochs
Orbit position	Integrated	2000 km	—
Orbit velocity	Process noise	2 km/s	0.54 cm/s (random walk)
Time tag	Random walk	100 s	0.5 s (random walk)
Pseudorange bias	White noise	300 km	300 km (white noise)
Clock rate	Process noise	1 μs/s	1 μs/s (white noise)

treating the previous UD matrix as a priori for starting the filter iteration. However, this would tend to put more weight on the new data batch as the number of iterations increases.

The user orbit-solution error components for the entire period are shown in Figs. 7 and 8. The filter orbit position errors are at integer multiples of a half-hour, when snapshots of data are taken. Between these half-hour points, the orbit prediction errors from the previous data epochs are shown. The rms filter orbit errors for the first day (Fig. 7) are 19 m radial (H), 7 m cross-track (C), and 67 m in-track (L). The predicted orbit errors are slightly larger at 31 m (H), 8 m (C), and 75 m (L).

The large error for the predicted orbit near the beginning of the second day (Fig. 8) is due to a large velocity error as a result of using a single epoch of data for the orbit determination from a cold start. The filter orbit errors for the second day are 23 m (H), 15 m (C), and 98 m (L), and the predicted orbit errors (excluding the first 0.5 hour) are 33 m (H), 15 m (C), and 99 m (L). The velocity errors are about 0.1 m/s (H) and 0.01 to 0.03 m/s (C and L). The time-tag error is 10 to 20 ms.

These results indicate that an efficient data acquisition and filtering scenario is such that snapshots of GPS Doppler and ambiguous pseudorange measurements are taken every 30 min. At a cold start, two epochs of data are used for pseudorange ambiguity resolution as well as for orbit determination and prediction. Afterward, only a single epoch of data is used for orbit updating. To ensure stability at the cold start, it might be useful to employ several more closely spaced epochs of Doppler data with noise greater than 2 m/s.

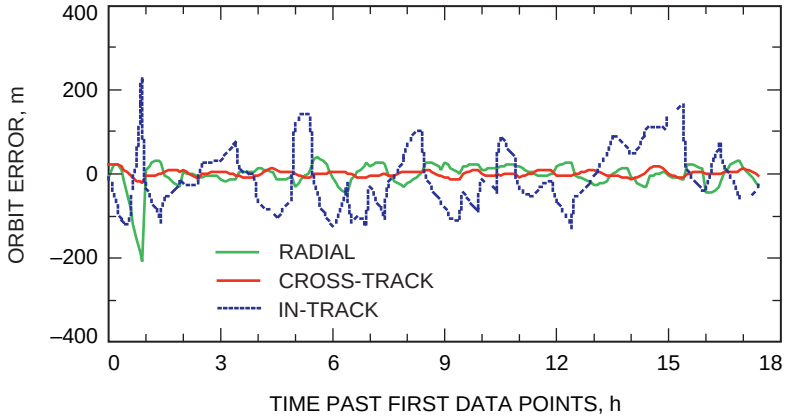

Fig. 7. Final orbit solutions for day 1.

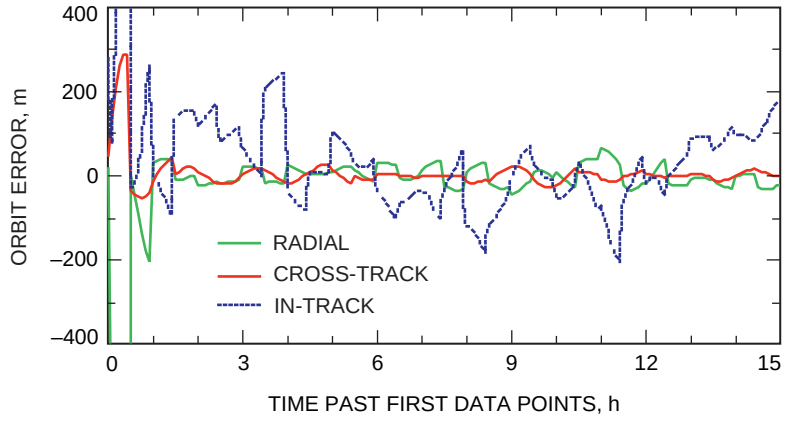

Fig. 8. Final orbit solutions for day 2.

IX. Summary

The feasibility of medium-precision orbit determination for a low Earth-orbiting satellite carrying a simple microGPS receiver has been demonstrated with 2 days of actual GPS data from the GPS/MET satellite. The results of this demonstration indicate that snapshots of GPS carrier Doppler and ambiguous pseudorange measurements taken every 30 min are sufficient to maintain the orbit within a few hundred meters. Such sparse data acquisition is the key to ultra-low mass and power for the microGPS receiver. The few-hundred-meter orbit accuracy can be arrived at only with the pseudorange ambiguities resolved using the Doppler data. At a cold start, two epochs of data are used for pseudorange ambiguity resolution as well as for orbit determination and prediction. Afterward, only single epochs of data at a time are used for orbit updating.

The success of pseudorange ambiguity resolution depends on carrier Doppler data quality. Doppler data of 2- to 5-m/s quality are shown to be appropriate. On the other hand, the final orbit accuracy depends on the pseudorange data quality. We anticipate, based on the GPS/MET data demonstration, that the SNOE orbit can be determined to better than 100 m (1 σ) and 0.1 m/s (1 σ), and that the data time tag can be determined to better than 20 ms (1 σ).

References

[1] T. P. Yunck, S. C. Wu, J. T. Wu, and C. L. Thornton, "Precise Tracking of Remote Sensing Satellites With the Global Positioning System," *IEEE Trans. Geosci. and Remote Sensing*, vol. 28, no. 1, pp. 108–116, January 1990.

[2] M. Heflin, D. Jefferson, Y. Vigue, F. Webb, J. Zumberge, and G. Blewitt, "Site Coordinates and Velocities From the Jet Propulsion Laboratory Using GPS," *IERS Tech. Note 17*, p. P-49, 1994.

[3] T. P. Yunck, W. I. Bertiger, S. C. Wu, Y. E. Bar-Sever, E. J. Christensen, B. J. Haines, S. M. Lichten, R. J. Muellerschoen, Y. Vigue, and P. Willis, "First Assessment of GPS-Based Reduced Dynamic Orbit Determination on TOPEX/ POSEIDON," *Geophys. Res. Letters*, vol. 21, no. 7, pp. 541–544, 1994.

[4] W. I. Bertiger, Y. E. Bar-Sever, E. J. Christensen, E. S. Davis, J. R. Guinn, B. J. Haines, R. W. Ibanez-Meier, J. R. Jee, S. M. Lichten, W. G. Melbourne, R. J. Muellerschoen, T. N. Munson, Y. Vigue, S. C. Wu, T. P. Yunck, B. E. Schutz, P. A. M. Abusali, H. J. Rim, M. M. Watkins, and P. Willis, "GPS Precise Tracking of TOPEX/POSEIDON: Results and Implications," *J. Geophys. Res.*, vol. 99, no. C12, pp. 24,449–24,464, December 1994.

[5] W. Bertiger and S. C. Wu, "Single Frequency GPS Orbit Determination for Low Earth Orbiters," ION National Technical Meeting, Santa Monica, California, January 1996.

[6] W. I. Bertiger, Y. E. Bar-Sever, B. J. Haines, B. A. Iijima, S. M. Lichten, U. J. Lindqwister, A. J. Mannucci, R. J. Muellerschoen, T. N. Munson, A. W. Moore, L. J. Romans, B. D. Wilson, S. C. Wu, T. P. Yunck, G. Piesinger, and M. Whitehead, "A Prototype Real-Time Wide Area Differential GPS System," ION National Technical Meeting, Santa Monica, California, January 1997.

[7] G. J. Bierman, *Factorization Methods for Discrete Sequential Estimation*, New York: Academic Press, 1977.